

1 **PREPRINT: Predicting rut depth with sSoil moisture estimates modelling with**
2 **from ERA5-Land retrievals, topographic indices and in-situ measurements and its**
3 **use for predicting ruts**

4 Marian Schönauer¹, Anneli M. Ågren², Klaus Katzensteiner³, Florian Hartsch¹, Paul Arp⁴, Simon
5 Drollinger⁵, Dirk Jaeger¹

6 ¹Department of Forest Work Science and Engineering, University of Göttingen, Göttingen, Germany

7 ²Department of Forest Ecology and Management, Swedish University of Agricultural Sciences, Umeå, Sweden

8 ³Institute of Forest Ecology, University of Natural Resources and Life Sciences, Vienna, Vienna, Austria

9 ⁴Forestry and Environmental Management, University of New Brunswick, New Brunswick, Canada

10 ⁵Department of Physical Geography, University of Göttingen, Göttingen, Germany

11 *Correspondence to:* Marian Schönauer (marian.schoenauer@uni-goettingen.de)

12 **Abstract**

13 Spatiotemporal modelling is an innovative way of predicting soil moisture and has promising applications in
14 supporting sustainable forest operations. One such application is the prediction of rutting, since rutting can cause severe
15 damage to forest soils and ecological functions.

16 In this work, we used ERA5-Land soil moisture retrievals and several topographic indices to model ~~the response~~
17 ~~variable, variations of~~ in-situ soil water content, by means of a random forest model. We then correlated the predicted
18 soil moisture with rut depth from different trials.

19 Our spatiotemporal modelling approach successfully predicted soil moisture with a Kendall's rank correlation
20 coefficient of 0.62 (R^2 of 64%). The final model included the ~~topographic-spatial~~ depth-to-water index, ~~slope, stream~~
21 ~~power index,~~ topographic wetness index, stream power index, as well as temporal components such as ~~numeric~~
22 ~~variables derived from date and month and season, and~~ ERA5-Land soil moisture retrievals. These retrievals showed
23 to be the most important predictor in the model, indicating a large temporal variation. The prediction of rut depth was
24 also successful, resulting in a Kendall's correlation coefficient of 0.613.

25 Our results demonstrate that by using data from several sources, including ERA5-Land retrievals, topographic indices
26 and in-situ soil moisture measurements, we can accurately predict soil moisture and use this information to predict rut
27 depth. This has practical applications in reducing the impact of heavy machinery on forest soils and avoiding wet areas
28 during forest operations.

29 **Keywords:** spatiotemporal modelling, forest management, forest engineering, rutting, downscaling, reanalysis

30 **1 Introduction**

31 For decades, forestry research has sought solutions to accurately predict the trafficability of forest soils (Murphy et al., 2007;
32 White et al., 2012; Mattila and Tokola, 2019). In order to further sustainable forest management, efficient protection of forest
33 soils is mandatory (Vega-Nieva et al., 2009; Uusitalo et al., 2019; Picchio et al., 2020). Heavy harvesting and forwarding
34 machines have been frequently associated with severe soil damage, particularly when operating on soils with low bearing

35 capacity (Horn et al., 2007; Allman et al., 2017). Soil compaction ~~as-is a common~~ consequence of harvesting operations
36 (Eliasson, 2005; Ampoorter et al., 2010; DeArmond et al., 2021) ~~is-and has shown to be~~ detrimental to a number of ecological
37 functions, including soil biota (Beylich et al., 2010), hydrological patterns, and nutrient supply, with potential drawbacks on
38 plant growth and site productivity (Curzon et al., 2022). In addition to soil compaction, machine traffic can also result in deep
39 ruts (Horn et al., 2007; Poltorak et al., 2018; Ala-Ilomäki et al., 2021), which affect site hydrology and increase anaerobic
40 conditions at the rut's base, where air-filled porosity is reduced, leading to minimized soil aeration (Hansson et al., 2019).

41 -The risk of causing high degrees of soil compaction and rutting is mainly attributed to soil properties such as initial soil bulk
42 density and texture, as well as the current soil water content (Cambi et al., 2015; Crawford et al., 2021). Moist soils show a
43 higher susceptibility to damage since the internal friction is decreased through water embracing soil particles (Hillel, 1998),
44 reducing the soil bearing capacity and the ability for elastic responses to machine-induced impacts (McNabb et al., 2001).

45 To support forestry management and machine operators, accurate cartographic information on soils with low bearing capacity
46 is essential (Campbell et al., 2013; Jones and Arp, 2017; Sirén et al., 2019). However, existing models that rely on detailed
47 soil maps to retrieve soil mechanical parameters (e.g. Gröll, 2011; Heubaum, 2015) require a high level of input data, and
48 high-resolution soil maps are only available for selected areas, hindering their large-scale application (Vega-Nieva et al.,
49 2009; Kristensen et al., 2019). Therefore, researchers have turned to topographic modelling as a more promising approach
50 (White et al., 2012; Lidberg et al., 2020), as it requires only digital elevation models (DEM), which are increasingly available
51 for most parts of Europe (Guo et al., 2017; Hoffmann et al., 2022). One topographic index that has been extensively studied
52 is the "depth-to-water" (DTW) concept, originally developed and tested at the University of New Brunswick by Meng,
53 Ogilvie, and Arp, as described by Murphy et al. (2007; 2009). The DTW concept calculates flow lines across areas of interest
54 by determining a flow accumulation and selecting lines that originate at a set threshold of accumulated upstream contributing
55 areas. Using a cost function that considers the cell-to-cell slopes, the vertical distances from each cell within a raster to the
56 nearest simulated flow line are ascertained. DTW is well documented (e.g. Vega-Nieva et al., 2009; Murphy et al., 2011;
57 White et al., 2012).

58 Previous research has shown that the DTW index performs relatively well in predicting wet areas in forested formerly
59 glaciated landscapes compared to other indices (Ågren et al., 2014; Larson et al., 2022). Recent studies have explored further
60 developments in moisture prediction by utilizing machine learning algorithms applied to a variety of freely available data and
61 diverse retrieved information, including different topographic indices calculated on DEMs. Ågren et al. (2021); used 28
62 topographic predictor variables in an eXtreme Gradient Boosting model (Chen et al., 2021) to predict soil moisture across the
63 entire Swedish forest landscape at high resolution (2x2 m). Although topographic modelling approaches are widely used, they
64 often fail to adjust to seasonal changes in soil water regimes. Static maps may not adequately represent temporal occurrences
65 of flow lines, wet fields, or water-saturated soils. To address this issue, the DTW concept offers a potential solution, enabling
66 the calculation of different scenarios ranging from 'very dry' or 'frozen' to 'wet' soil conditions. However, selecting the most
67 accurate DTW scenario requires high expertise (Leach et al., 2017; Lidberg et al., 2020), and mistakes can lead to reduced
68 accuracy and result in potential soil damages that could be avoided.

69 Therefore, we believe that the next crucial step in soil moisture modelling is to incorporate a temporal component that enables
70 the prediction of rasters for any given time and area. One approach to achieve this was designed by Schönauer et al. (2022),
71 who developed a spatiotemporal prediction model. Dynamic satellite-based retrievals of soil moisture with coarse spatial
72 resolution (Soil Moisture Active Passive Mission) were combined with high-resolution but static topographic maps. This

73 resulted in improved performance in predicting moisture values across time-series conducted on sites in Finland, Germany,
74 and Poland. The incorporation of a dynamic component into the prediction model enabled reflection of the current overall
75 moisture conditions on the study sites. This allowed to calculate daily prediction grids that could support forestry practice and
76 enable the guidance of machine operators on sites to avoid traffic on wet areas susceptible to damages. However, a validation
77 of predicting rut depth by models of this kind has not been facilitated yet.

78 The effectiveness of soil moisture modelling, whether based on static or dynamic independent variables, is ultimately
79 constrained by the quality of the dependent variable, which in this case is in-situ soil moisture. Manual measurements of soil
80 moisture have been conducted in numerous studies using different devices, such as hand-held time-domain reflectometry
81 sensors (Kemppinen et al., 2018; Uusitalo et al., 2019) or impedance measuring techniques (e.g. Schönauer et al., 2021b).
82 Despite the potential inaccuracies associated with these techniques (Walker et al., 2004; Francesca et al., 2010), they offer
83 significant advantages in terms of flexibility, scalability, low investment costs, and minimal maintenance. Another option is
84 the use of continuously measuring sensor networks (e.g. Oliveira et al., 2021), which can provide relatively reliable
85 measurements but with limited spatial coverage due to the high costs of installation and maintenance.

86 In this study, we built upon the approach developed by Schönauer et al. (2022) by incorporating additional data sources,
87 including additional topographic indices, soil maps, and soil moisture retrievals from ERA5-Land for two soil depths. The
88 study also used two types of data sources for soil moisture measurements: manual measurements using a handheld moisture
89 meter, and data from two continuously measuring sensor networks. We argue that manual measurements are simpler and can
90 be applied to larger areas, while sensor networks are more expensive and limited to chosen positions.

91 The study had two main objectives: 1.) to train soil moisture models using the two individual data sets (manual measurements
92 and sensor networks) and evaluate their prediction performance, and 2.) to select the best combination of predictor variables
93 (e.g. topographic indices, ERA5-Land values) using a repeated cross-validation approach and compare the best models with
94 rut depth data obtained during four trials using a forwarder.

95 **2 Material and Methods**

96 To model soil water content (SWC), random forest models were trained using two separate datasets: manual in-situ
97 measurements using an impedance measuring technique (IMT) and continuously measuring soil sensor networks (SSN). To
98 both datasets we added predictor variables derived from topographic indices (e.g. depth-to-water, topographic wetness index),
99 soil maps, SWC estimates from the ERA5-Land campaign (SWC_{ERA}), and numerical values for date (month and season). We
100 performed cross-validation and reduced features stepwise to choose the best-performing model. Subsequently, the two final
101 models (for IMT and SSN) were used to predict SWC for the positions and dates of different field trials with a forwarder.
102 During this field trials, rut depth data was captured, and compared to the predictions from the final SWC-models (Figure 14).

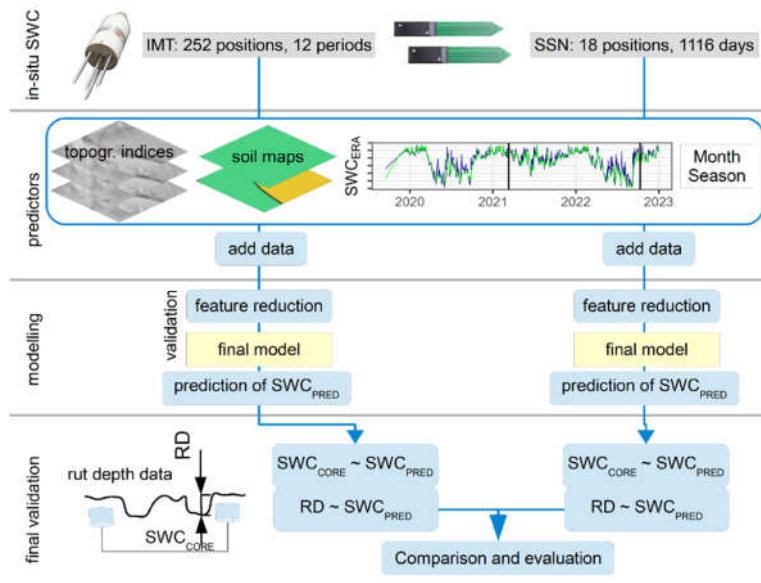


Figure 1: Soil water content (SWC, [%]) was predicted using models trained on two datasets: in-situ measurements (IMT) and soil sensor networks (SSN). Input variables included topographic indices, soil type data, SWC estimates from ERA5-Land (SWC_{ERA}), and date values. Through cross-validation, we selected the final models, used to predict SWC_{PRED} for various positions and dates during trials with a forwarder. Model estimates were compared with in-situ SWC_{CORE} and rut depth (RD, [cm]).

1.12.1 Study sites

The data acquisition of volumetric soil water content (SWC_v [%]) and the trials with a forwarder were conducted in two forest stands located near the city of Arnsberg in North Rhine-Westphalia (Figure 2). The forest stands were situated at an altitude of approximately 250 m on common soil types such as Cambisol and Stagnosol on Claystone and Sandstone from Devon and Carbon (Table 1).

Table 1. Characteristics of the study sites, where soil water content was captured and field trials with a forwarder were performed.

Site	Coordinates in WGS84		Dominant soil types	Humus form	Slope [%]	Canopy
	x	y				
<u>1A</u>	8.039	51.406	Cambisol - Stagnosol	Mesomull	15-30	<i>Fagus sylvatica</i> , <i>Quercus spp.</i> , <i>Pinus sylvestris</i>
<u>2B</u>	8.024	51.473	Stagnosol	Mull	1-7	<i>Fagus sylvatica</i>

We collected SWC data through manual measurements and a continuously measuring soil sensor network. By merging this data with various topographic indices, soil maps and temporal retrievals, we created spatiotemporal models of SWC, which were validated through repeated cross validation. These models were then used to predict rut depth estimated during four field trials (details in Sect. 2.2).

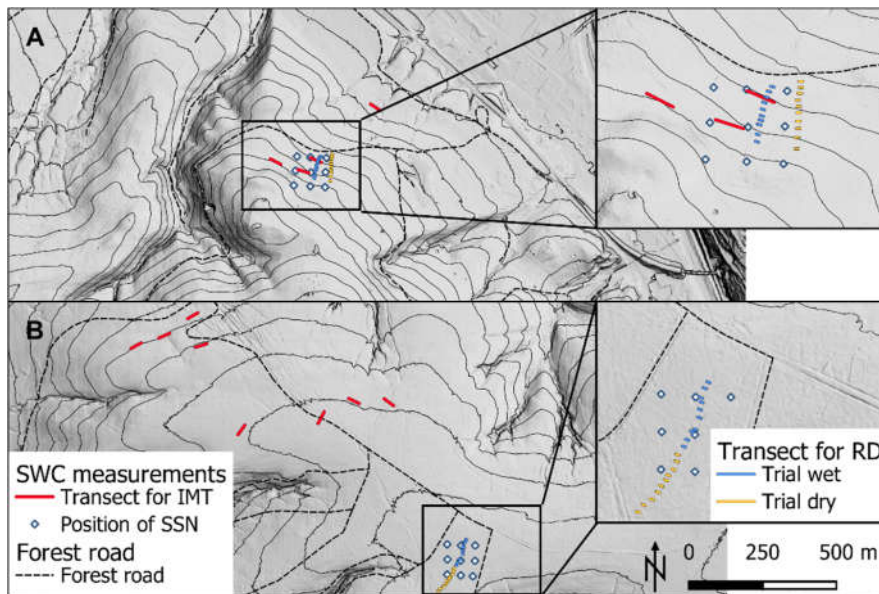


Figure 2: The map indicates the locations of two experimental areas on a hill-shaded digital elevation model with 10 m contour lines; Site A (A, coordinates x, y in WGS84: 8.039, 51.406) and Site B (B, coordinates: 8.024, 51.473), which were used for collecting time-series data on soil water content (SWC). SWC was measured using a handheld soil moisture meter (impedance measuring technique, IMT) along transects (red lines), each containing 21 measuring positions (2 m spacing). In addition, a soil sensor network (SSN) was used to continuously capture SWC at 18 positions (white rhombus). The map also indicates the locations of 40 transects (in crop-outs) used for measuring rut depth (RD) during relatively wet conditions (Trial_{WET}, blue lines) and dryer conditions (Trial_{DRY}, orange lines).

1.2.2.2 Soil moisture models

1.2.2.2.1 In-situ soil moisture measurements

Two sets of in-situ data of soil moisture were used: 1. Manual measurements of SWC were performed using a HH2 Moisture Meter (Delta-T Devices Ltd, England), which applies Impedance Measuring Technique (i.e. 'IMT') (Eijkelkamp Agrisearch Equipment, 2013). These measurements were saved in the dataset 'IMT' 2. In addition, data from a continuously measuring Soil Sensor Network (i.e. 'SSN') was used, giving the dataset 'SSN'.

The IMT data used for this study were previously used for the validation by Schönauer et al. (2022) and consisted of 12 measuring transects. The transects were placed in various positions in broadleaved forests, known to be temporarily wet or sensitive for machine traffic, with each transect having a length of 40 m. SWC was measured with a spacing of 2 m along the transects. To measure SWC, measuring rods of 60 mm length were vertically inserted into the soil after removing the humus layer. The measurements were taken almost monthly between September 2019 and October 2020 (Figure 3B). The IMT data consisted of 2,184 observations. Overall, this dataset offers a relatively high level of spatial granularity, with 252 measuring positions. However, the temporal resolution of the data is relatively low, with only monthly measuring campaigns conducted. The SSN was launched in Dezember 2019 and its data was obtained from continuously measuring SMT100 sensors (TRUEBNER GmbH, Germany), placed on two sites, each having 9 positions with a spacing of 50x50 m. These sites were specifically selected because they were known to be temporarily wet or sensitive for machine traffic. At each position, two sensors were placed at a depth of 10 cm in the mineral soil, with a temporal resolution of 15 minutes. The data from these sensors were averaged for each position and each of the 1,116 days captured (data until 2022-12-31 was included), resulting in a total of 16,351 observations after omitting all missing values. While this data set provides a high level of temporal

134 granularity, it suffers from a low level of spatial granularity due to the limited number of positions sampled.
135 To enable the incorporation of seasonal effects in the modelling approaches, we transformed the date of each measurement
136 into numeric vectors, resulting in the variables ~~Year~~, ~~Month~~, and Season. The coding used for Season was as follows: 1 for
137 March, April, and May; 2 for June, July, and August; 3 for September, October, and November; and 4 for December, January,
138 and February.

139 To enable the creation of spatiotemporal data, the positions of all measuring locations were captured using post-processed
140 signals from a GNSS device (Trimble R2 RTK Rover, Trimble, Colorado, USA). This data was then fused with a range of
141 topographic indices. To achieve this, values of several topographic indices were extracted at each measuring position of IMT
142 and SSN ~~and inserted into the attributes of a shapefile.~~

143 1.2.22.2.2 Topographic indices

144 For calculating topographic indices, we used a freely available digital elevation model (DEM), as provided by the
145 Bezirksregierung Köln (2020). The resolution of this model was 1x1 m, with a vertical accuracy of ± 0.2 m. Using the free
146 programming language R (version 4.0.2, R Core Team, 2023) and RStudio (version 2022.07.2, Posit PBC, Massachusetts,
147 USA), along with the package "rgrass" (Bivand, 2021) to utilize GRASS GIS (Awaida and Westervelt, 2020) commands in
148 the R interface, the command 'r.hydrodem' was used to 'remove all sinks' (Flags: -a) from the DEM. Thereafter, we calculated
149 depth-to-water (DTW) maps. To generate these maps, we followed the script by Schönauer and Maack (2021) and used flow
150 initiation areas (FIA) of ~~varying the following~~ sizes (0.25 ha (DTW025), 1.00 ha (DTW1), and 4.00 ha) (DTW4), ~~which to~~
151 ~~account for different overall soil moisture conditions. The DTW maps were named DTW025, DTW1, and DTW4,~~
152 ~~corresponding to the FIA used.~~ A smaller FIA result~~ed~~ in a DTW map for wetter conditions, as the network of simulated
153 flow lines expand~~ed~~, while a larger FIA represent~~ed~~ drier conditions. For further details, refer to Murphy et al. (2009; 2011).
154 The Topographic Wetness Index (TWI) represents the tendency for water to accumulate at any point in the catchment (Quinn
155 et al., 1991), while the stream power index (SPI) represents the power of water flow at any point in the catchment and the
156 gravitational forces that move water downslope (Moore et al., 1991). To compute TWI, we used the 'r.watershed' command
157 in GRASS GIS, as conceived by Sørensen and Seibert (2007). TWI was calculated as $\ln(\alpha/\tan(\beta))$, where α is the cumulative
158 upslope area draining through a point per unit contour length, and $\tan(\beta)$ is the local slope angle. SPI (Moore et al., 1991) was
159 calculated as $\alpha * \tan(\beta)$ (Moore et al., 1991). Flow Accumulation, representing the absolute amount of overland flow passing
160 through each cell, ~~and Basin, indicating the watershed basin with a threshold of 0.25 ha, were~~ was also included as a variable.
161 TWI, SPI, and Flow Accumulation were calculated on an aggregated DEM with a spatial resolution of 15x15 m. This
162 resolution has been shown to exhibit a stronger correlation with SWC, and can be assumed to be more robust (Ågren et al.,
163 2014), ~~as observed in prior work where resolutions ranging from 1 to 20 m were tested (data not shown).~~ In addition, we
164 calculated the variable Slope [°] using the R-package 'raster' (Hijmans, 2020).

165 1.2.32.2.3 Soil maps

166 Soil maps of North Rhine-Westphalia were originally generated at a scale of 1:5,000 from forest site surveys. We included
167 soil type information (Soil05) for the analysis. While these maps are not available across the entire region of North Rhine-
168 Westphalia, ~~we were able to gather them for~~ they were provided for the study sites by the Geological Survey of North
169 Rhine-Westphalia. Soil type from these soil maps was added as variable Soil05.

170 By contrast, soil maps with a scale of 1:50,000 are available for the entirety of North Rhine-Westphalia (Soil50). ~~We added~~
171 ~~the soil type information derived from these maps as Soil50.~~

172 1.2.4.2.4 Temporal soil water content from ERA5-Land

173 ERA5-Land is a global reanalysis dataset providing hourly estimates of meteorological variables at a spatial resolution of 9x9
174 km, including soil moisture [$\text{m}^3 \text{m}^{-3}$] ~~at the top soil layer. ‘Volumetric soil water layer 1’ [$\text{m}^3 \text{m}^{-3}$], one of the available~~
175 ~~parameters, represents the water content in the top soil layer~~ (0-7 cm, ‘layer 1’ (L1)) ~~and at a depth -of 7-28 cm (‘layer 2’~~
176 ~~(L2)). ERA5-Land data is~~ retrieved by assimilating satellite ~~and atmospheric forcing~~ (Muñoz-Sabater et al., 2021) ~~and ground-~~
177 ~~based observations. Soil water content for a depth of 7-28 cm is given by ‘Volumetric soil water layer 2’. It provides a reliable~~
178 ~~representation of soil moisture values and variations across the majority of global regions, making it applicable for various~~
179 ~~geophysical applications~~ (Lal et al., 2022).

180 ~~To gather data from ERA5-Land, w~~We utilized the API provided by CDS (Copernicus Climate Change Service, 2019) and
181 the R-package 'ecmwf' (Koen Hufkens et al., 2019) to download daily grids (at 14:00 UTC) of layer 1 and 2. The downloaded
182 data covered both the ~~whole time span of our data and the two~~ measuring ~~positions sites~~ ~~and time span required for the analysis.~~
183 ~~Both sites were situated in one 9x9 km raster cell of the ERA5-Land. The land cover for this cell was derived from~~
184 ~~Bezirksregierung Köln (2023), showing that open land (e.g. grassland, crops) dominated with 52% of the total cover, whereas~~
185 ~~forests occurred on approximately 31% of the cell size, followed by 12% coverage from infrastructure, 3% loose material,~~
186 ~~and 2% water bodies.~~

187 After downloading the data, we stacked the daily grids and extracted the corresponding values at each measuring position,
188 giving $\text{SWC}_{\text{ERA}L1}$ ~~and~~ $\text{SWC}_{\text{ERA}L2}$, ~~respectively.~~

189 All data, the topographic information, soil types, numerical values of date and the dynamic variables from ERA5-Land were
190 merged with in-situ data, either IMT or SSN.

191 1.2.5.2.5 Modelling

192 The modelling approach described here was applied separately for both data sets, IMT and SSN (the main outputs when both
193 datasets were combined can be seen in Appendix A).

194 Initially, we fitted a linear model with SWC as the dependent variable and $\text{SWC}_{\text{ERA}L1}$, $\text{SWC}_{\text{ERA}L2}$, ~~Year~~, Month, Season,
195 DTW025, DTW1, DTW2, DTW4, Slope, TWI, SPI, Accumulation, ~~Basin~~, Soil05, and Soil50 as the independent variables.
196 We then used this linear model to check the data for autocorrelations and subsequently eliminated variables with a variance
197 inflation factor > 10 through an iterative process, reducing one variable at a time. Also, the feature selection according to the
198 Boruta algorithm (package 'Boruta', Kursa and Rudnicki, 2010) was applied.

199 We then trained random forest models (Breiman, 2001), repeatedly reported as efficient in predicting complex data
200 (Kemppinen et al., 2018; Carranza et al., 2021; Cavalli et al., 2023), using the 'ranger' package (Wright and Ziegler, 2017)
201 with a 10-fold cross-validation with 5 repetitions. For each of the 50 models in the validation of ~~a model one configuration,~~
202 we noted the mean ~~of Kendall’s coefficient of correlation~~ R^2 ~~(according to Kuhn (2020))~~ τ ~~(since different sample sizes~~
203 ~~occurred)~~ of the random forests and the representative standard deviation. In addition, the least important variable according
204 to impurity and its frequency within the 50 validation sets were traced. The variable noted most frequently as least important
205 was then removed, and a new cross-validation was performed on $\text{SWC} \sim (n-1)$ variables, with n being the number of predictors

206 in the model trained previously. This process was repeated until only one predictor variable remained.
207 To avoid temporal autocorrelations at the measuring positions, positions IDs were used to select the folds of the cross
208 validations.

209 **2.2.6 Selection of the final model**

210 To select the final random forest model for each data partition, we examined the maximum τ values obtained and multiplied
211 them by 0.99 (according to Hauglin et al. (2021)). This was done to penalize the use of an unnecessarily high number of
212 predictor variables. We selected the model with the least number of predictor variables within this 1%-range as the final
213 model. The final models (built on IMT and SSN data) were then used to predict rasters of SWC_{PRED} , which were visually
214 evaluated. Subsequently, the outputs of the final models were compared to rut depths and SWC at the machine operating
215 trails.

216 **2.3 Rut depth data**Data from field trials with a forwarder

217 **2.3.1 Rut depth (RD)**

218 During the field trials conducted in two forest stands at two seasons, a fully loaded forwarder (John Deere 1210G, 8-Wheel
219 model, total mass of 28 Mg (18 Mg machine weight + 10 Mg loading)) was used. The first trial was conducted on section 1
220 of an existing machine operating trail on 2021-03-11, during generally wet conditions ($Trial_{\text{WET}}$), and Tthe second trial was
221 conducted on subsequent section 2 of the same machine trail on ~~2020~~2022-10-11, during dryer conditions ($Trial_{\text{DRY}}$) (Figure
222 2, Site A), or in close proximity of section 1 (~~Figure 1~~Site B), as there the machine trail was not long enough for both sections.
223 The four trials were positioned near the sensors of the SSN (Figure 2) and, in the case of Site A, near the IMT measuring
224 transects. On Site B, the IMT transects were at a distance of 530 m to 1300 m. Moreover, there is a temporal lag between the
225 IMT measuring campaigns and the field trials (Figure 3). This discrepancy stems from the IMT data being collected as part
226 of a separate research project.

227 The 8-wheel machine, ~~with a constant total mass of 28 Mg (18 Mg machine weight + 10 Mg loading),~~ trafficked section 1
228 and 2 of both operating trails, and made four passes.

229 Before the first machine pass, the initial surface was captured along 10 perpendicular transects on each of the four sections.
230 These 4 m wide transects, ~~which were 4 m wide,~~ were placed and marked permanently with inserted wooden pegs. The same
231 pegs were used to position the beam, which served as the reference height to measure profiles along each transect. Into this
232 beam, metric scales were inserted with a spacing of 10 cm in between, to note the distance between the surface and the beam
233 to the nearest cm. These measured distances (D_0 , [cm]) describe the surface along the transect on already existing machine
234 operating trails, prior to the trial conducted in this study. The same procedure was repeated after the fourth consecutive
235 machine passes, giving D_4 [cm].

236 Next, the differences between D_0 and D_4 were calculated at each of the 41 measurements (10 cm spacing over 4 m) along a
237 transect. The maximum value of these differences, measured at the left or right machine track, was used to determine rut depth
238 (RD , [cm])~~[cm]~~. We used average values of both tracks to prevent pseudo replicates, since intraclass correlation coefficient
239 was high (0.83), when left and right tracks were integrated separately. Moreover, mean and maximum values of rut depth
240 were highly correlated (adj. $R^2 = 0.96$).

241 **2.3.2 Soil water content at the rut depth transects (SWC_{CORE})**

242 Volumetric soil moisture content was captured outside the 1st, 4th, 7th and 10th transect of each section, with a distance of 1 m
 243 to the left and right track, at a depth of 10-15 cm. This water content was determined using 100 cm³ cores taken with an
 244 undisturbed core sampler, with three replicates at each measurement. SWC_{CORE} was calculated according to equation (1):

$$SWC_{CORE}[\%] = \frac{M2 - M1}{M1} * 100 \quad (1),$$

245 with M2 being the fresh mass of the soil taken with undisturbed cores and M1 being the mass after drying the samples in oven
 246 with 105 °C, until mass constancy was reached.

247 Measurements of RD and SWC_{CORE} were georeferenced using the GNSS devise and complemented with all the predictor
 248 variables, as described above.

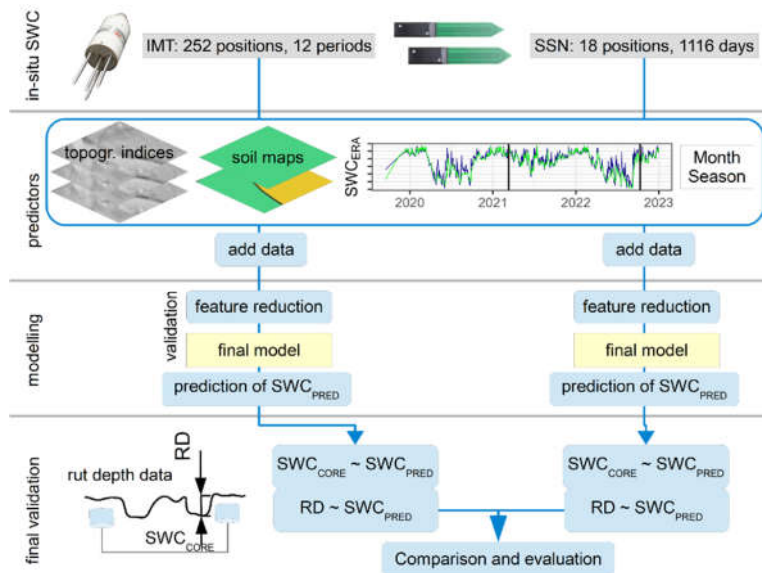
249 **2.4 Comparisons between model predictions and RD or SWC_{CORE}**

250 For the 'testing on rut depth data' (Figure 1), ~~Y~~ values of SWC_{PRED} were compared to RD or soil water content, captured
 251 through undisturbed cores along the transects, SWC_{CORE}. Therefore, the predictor variables ~~added to the~~ from the rut depth
 252 RD dataset were used to predict SWC_{PRED} by means of the final random forest models created in the soil moisture modelling.

253 ~~⊕~~ Since the goodness-of-fit between in-situ values of RD or SWC_{CORE} and SWC_{PRED} was to some degree sensitive to the seed
 254 set during modelling, we repeated the predictions ten times and used average values to receive robust estimates of SWC_{PRED}.

255 ~~In addition, to ascertain the quality of all models in predicting rut depth, RD was compared to SWC_{PRED} for each model during~~
 256 ~~the feature reduction.[NOTE: This has been done in earlier stages of the work, but was removed later]~~ To test the correlations

257 between paired samples of SWC_{CORE} or RD and SWC_{PRED}, Kendall's rank correlation was used. We illustrated the
 258 corresponding p-values as follows: '***' for p<0.001, '**' for 0.001-0.01, '*' for 0.01-0.05, (' ') for 0.05-0.10 and 'ns' for p-
 259 values being higher than 0.10. Values are given as mean±standard deviation.



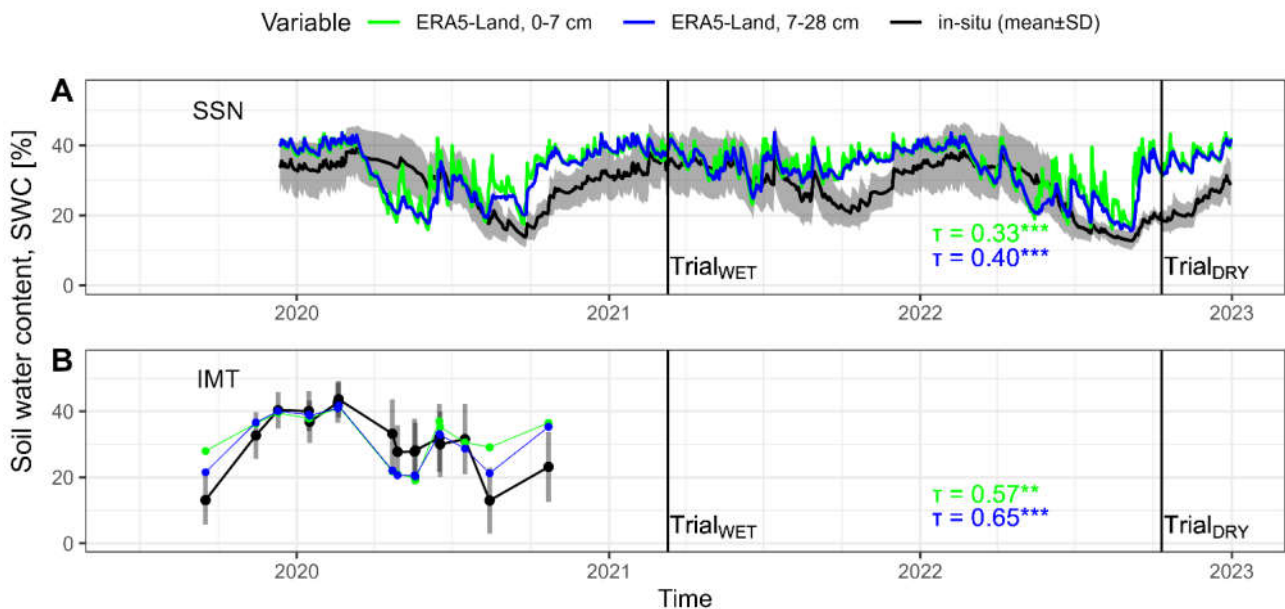
260 **Figure 2:** To predict soil water content (SWC, [%]), we trained models using two separate datasets: in-situ measurements using an impedance measuring technique (IMT) and continuously measuring soil sensor networks (SSN). The models used predictor variables derived from topographic indices (depth to water, topographic wetness index, stream power index, basin), soil maps (at 1:5,000 and 1:50,000 scales), SWC estimates from the ERAS Land campaign (SWC_{ERA}), and numerical values for date (month and season). We performed cross validation and reduced features stepwise to choose the best performing model, which was then used

to predict SWC for the positions and dates of different trials with a forwarder. SWC_{CORE}, measured in advance of the trials using undisturbed cores, and rut depth (RD, [cm]) were compared to model estimates from the final models of both datasets (IMT and SSN).

261 23 Results

262 2.13.1 Soil water content

263 Soil water content (SWC) was measured using a handheld moisture meter (IMT) during a field campaign launched in August
 264 2020. The mean value of SWC, measured using a handheld moisture meter (IMT), varied between 13.0±10.0% in August
 265 2020 and 43.2±5.95% in February 2020 (Figure 3). Daily mean values obtained from soil sensor networks (SSN) were similar
 266 to those obtained from IMT, ranging from 13.8±2.90% in September 2020 to 39.1±6.66% in March 2020, in the period that
 267 corresponds to the one covered by IMT. The driest conditions were observed in September 2022, with a daily mean SWC of
 268 12.7±2.55%. Overall, the results suggest that IMT and SSN provide comparable estimates of SWC, with the latter providing
 269 higher temporal resolution at a low spatial granularity.

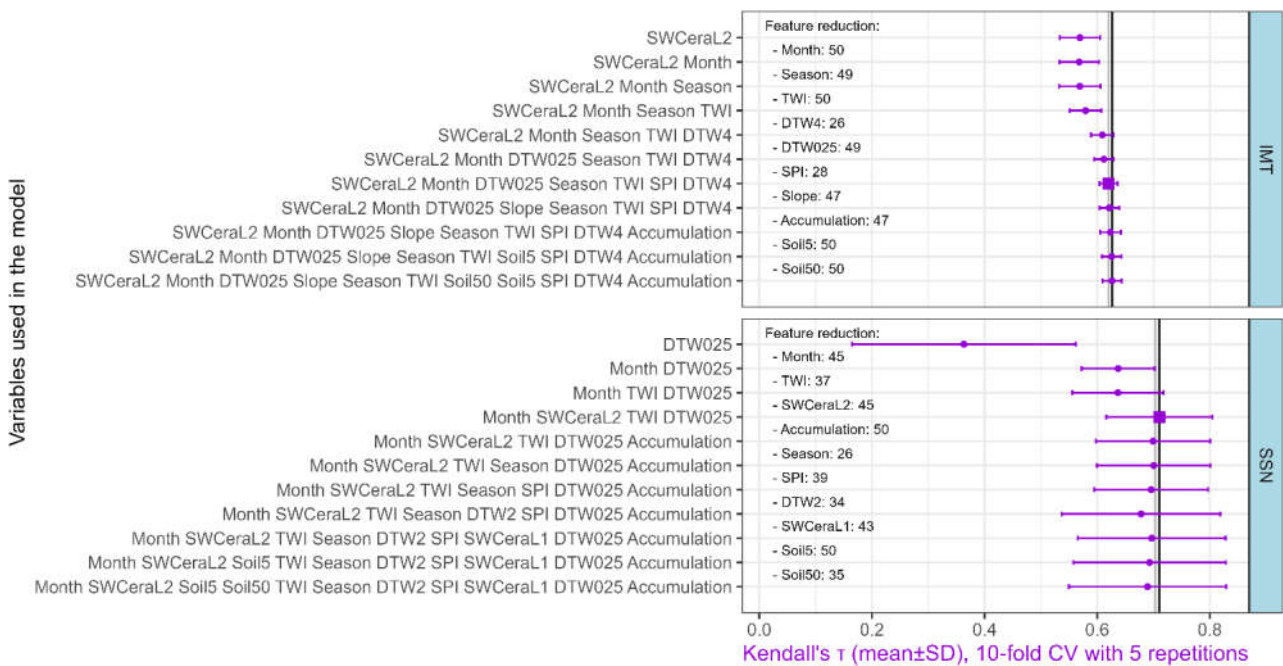


270 Figure 3: The figure displays time series of soil water content (SWC) measured using a soil sensor network SSN (A) with 18
 271 measuring positions on two sites and manual measurements using impedance measuring technique IMT (B) conducted on 252
 positions (black lines/points show daily mean values, grey shading/lines-bars show standard deviation for each day). SWC retrievals
 from ERA5-Land are shown as a blue line/point (0-7 cm vertical resolution-layer 1, as available from Copernicus Climate Change
 Service (2019)) and a green line/point (layer 2-7-28 cm vertical resolution). The goodness-of-fit between daily means of measured
 SWC and ERA5-Land retrievals is reported using Kendall's rank correlation coefficient (τ). Vertical lines indicate the dates of the
 trials when a forwarder conducted four passes at existing machine operating trials. Add IMT and SSN to the graph? like in fig 4?

272 2.23.2 Soil moisture models

273 The positions IDs were used to select the 10 folds for cross-validation. However, the dataset SSN had only 18 measuring
 274 positions (where SWC was measured on 1116 days), resulting in relatively high deviations of the resulting Kendall's τ R^2 of
 275 the random forests. The most important feature for this dataset was given by DTW025, although the resulting quality was

276 low, with ~~Kendall's coefficient of correlation~~ τ of 0.363 ± 0.198 . By adding the temporal component Month, the ~~Kendall's~~ τ
 277 improved to 0.637 ± 0.065 , which had the lowest standard deviation for the repeated folds. The final model for this dataset
 278 included ~~the temporal variables Month and SWC_{ERA}L2, as well as the~~ topographic predictor variables TWI ~~and, DTW2,~~
 279 ~~Accumulation, DTW025 and SPI, as well as temporal variables including Month, SWC_{ERA}L2, Year and Season~~ (Figure 4).
 280 The resulting τ was 0.71032 ± 0.095128 , revealed through the cross-validation.
 281 For the IMT partition, which had a low temporal but high spatial resolution, the most important feature was the temporal
 282 information SWC_{ERA}L2, leading to a τ of 0.581569 ± 0.03645 . The final model had an τ of 0.6202 ± 0.0168 , including the
 283 predictor variables SWC_{ERA}L2, Month, Season, and DTW025, ~~Slope, TWI, SPI, TWI~~ and DTW4.
 284 ~~Despite the low quality model for the SSN partition, in which DTW025 was used as only predictor variable, the τ values for~~
 285 ~~both partitions ranged from 0.581 ± 0.045 to 0.738 ± 0.128 , indicating a moderate level of predictability. Moreover, there was a~~
 286 ~~slight positive effect with an increase in the number of predictor variables (or "depth" of trees in the random forest).~~

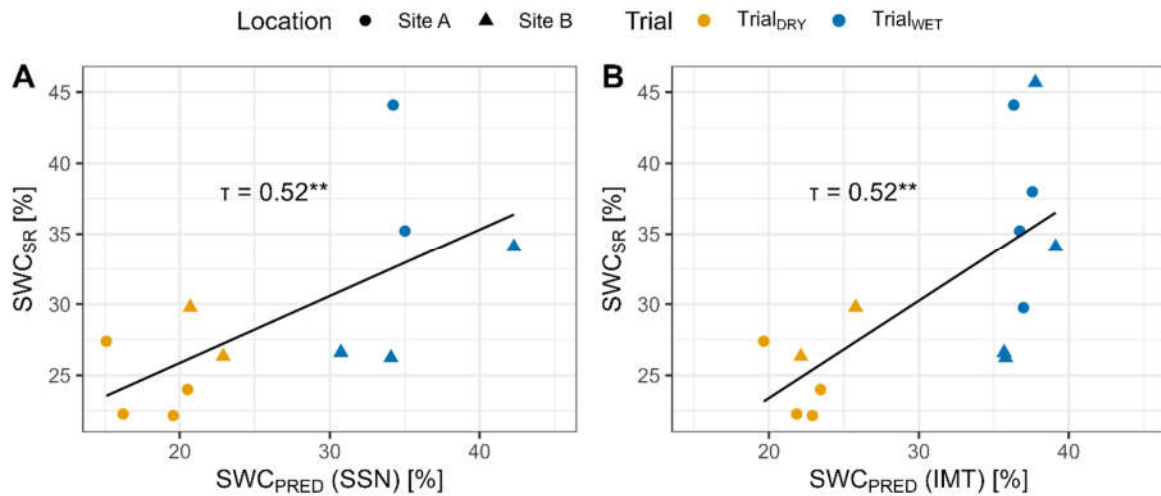


287

Figure 4: Soil water content (SWC) was modelled by random forests (RF), and evaluated by a repeated 10-fold cross validation (CV). Mean values and standard deviation of resulting values of the Kendall rank correlation coefficient τ during the CV are shown. A stepwise elimination of the least important variable was performed, and the frequency of this variable over all models is provided ("Feature reduction"). The vertical lines indicate the maximum value of τ (black) and the 99% of the maximum (grey), to select final models (squares). Variables used are described in section 2.

288 2.2.13.2.1 Comparisons of SWC_{CORE} with SWC_{PRED}

289 The final random forest models of both, the IMT and SSN dataset, were used to calculate SWC_{PRED} on the predictor variables
 290 of the rut depth data, including ~~the soil water content~~ SWC_{CORE} measured at the outside of a subsample of the measuring
 291 tracks by undisturbed cores. The comparison between SWC_{CORE} and SWC_{PRED} values predicted by the final random forest
 292 models of both datasets (SSN and IMT), revealed a significant association (Figure 5).



293

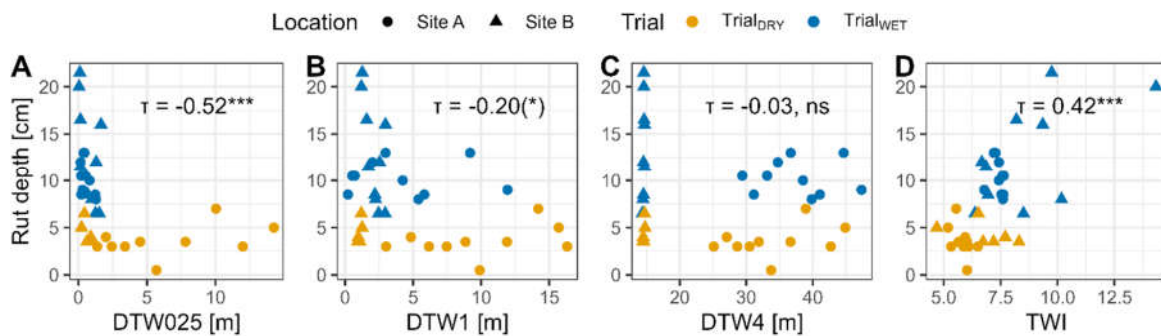
Figure 5: Soil water content was measured during two trials with a forwarder along a machine operating trail (n=14), using 100 cm³ undisturbed cores (SWC_{CORE}), and compared to values predicted (SWC_{PRED}) by a model trained data from a continuously measuring soil sensor network (SSN, A), or manual measurements with a handheld moisture meter (IMT, B). Correlations were evaluated using Kendall's τ and significance levels are indicated by *** for p<0.001, ** for 0.001-0.01, * for 0.01-0.05, (*) for 0.05-0.10, and 'ns' for p>0.10.

294 **2.3.3.3 Interrelations between Rut depth data and topographic indices or SWC**

295 Rut depth (RD, [cm]) was measured during four trials with a forwarder, covering 10 transects for each trial. This provided us
 296 with the potential for 40 measurements, but unfortunately, 4 of them were not ascertainable as the forwarder destroyed the
 297 wooden pegs that positioned the reference beam. In Trial_{WET-1}, conducted in March 2021, SWC_{ERA L1} and SWC_{ERA L2}
 298 showed a soil moisture level of 39%. At Site A1, the measured RD was 10.3±1.9 cm, while at Site B2, the RD was 12.7±5.5
 299 cm, with the highest value of RD recorded after 4 passes, with a depth of 21.5 cm. In Trial_{DRY-2}, conducted in October 2022,
 300 the soil water content from ERA5-Land was 32%. At Site A1, the measured RD was 3.5±1.7 cm, and at Site B2, the RD was
 301 4.3±1.2 cm.

302 **2.3.3.3.1 Comparisons of RD with DTW and TWI**

303 Considering the significance of the topographic indices DTW and TWI in the development of the SWC models (Figure 4),
 304 we aimed to compare RD with both indices. Notably, RD exhibited a clear correlation with DTW025, the most conservative
 305 DTW scenario (Figure 6). TWI also demonstrated a correlation with RD.



306

Figure 6. Rut depth (RD) was determined after four passes of a forwarder, driving on two Sites (A1 and B2), during two

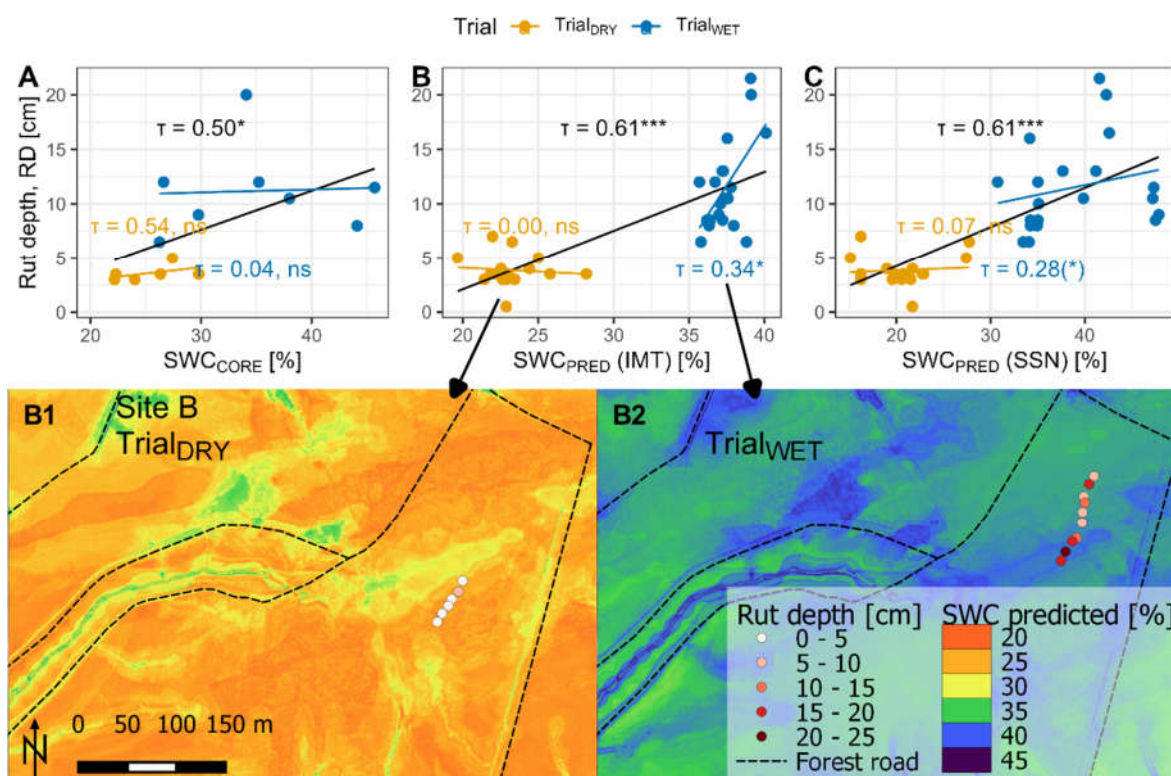
seasons conditions (Trial_{WET1} and Trial_{DRY2}). RD was compared to the topographic indices depth-to-water (DTW), calculated with different flow initiation areas (0.25 – 4.00 ha), and the topographic wetness index. Correlations were evaluated using Kendall's τ and significance levels are indicated by *** for $p < 0.001$, ** for 0.001-0.01, * for 0.01-0.05, (*) for 0.05-0.10, and 'ns' for $p > 0.10$.

While showing significant correlations, the nature of these static maps does not allow for the representation of current moisture conditions. This limitation was overcome when using the predicted (or observed) values of SWC.

2.3.2.3.2 Comparisons of RD with SWC_{CORE} and SWC_{PRED}

RD was positively correlated with SWC_{CORE} when both trials with different moisture conditions were included in testing (Figure 7A). However, when each trial was tested separately, no correlation between RD and SWC_{CORE} was observed. Compared to the correlation between RD and SWC_{CORE}, modelling outputs SWC_{PRED} proved to be a better predictor of rut depth, particularly for Trial_{WET1}. The final models that were selected for both datasets produced a Kendall's τ ~~coefficient~~ of 0.613 (for IMT, Figure 7B, ~~Figure 8~~) and 0.64 (for, and SSN, Figure 7C), when comparing RD of the four trials with the corresponding SWC_{PRED}. Although the R^2 values for these models were in similar range (0.62060 for IMT and 0.54965 for SSN), we chose to use Kendall's τ since different sample sizes were involved in the analysis. This was particularly relevant for comparing RD with SWC_{PRED} for each Trial separately. While no correlation could be found for Trial_{DRY2}, ~~performed during dryer conditions~~, correlations were found for ~~rut depth data of~~ Trial_{WET1}, with Kendall's τ of 0.3445 ($p=0.0374$) and 0.28132 ($p=0.09054$), for the final models trained on IMT and SSN, respectively (Figure 7B,C). Yet, these correlations seem to fragile, as a difference of a few percent of predicted SWC_{PRED} (IMT) is associated with the range of RD between 6.5 and 21.5 cm. Moreover, when analysing the sites separately, a vague trend between SWC_{PRED} and RD could be observed, but without showing significant correlations (Appendix B).

Since the final model trained on IMT data performed slightly better in Trial_{WET1} compared to the model trained on SSN data (Figure 7), we chose the IMT model for the generation of prediction rasters for the days of interest (Figure 7B1,B2).



326

Figure 7: Rut depth (RD) was determined after four passes of a forwarder, driving on two Sites (1 and 2), during two seasons conditions (Trial1 and Trial2_WET and DRY). RD was compared to SWC values, determined for undisturbed soil cores (A) and SWC values predicted by a random forest model trained on manually obtained IMT measurements (B, see Figure 1) and predicted by a model trained data from a continuously measuring soil sensor network (SSN, C). Correlations were evaluated using Kendall's τ . The correlation of all values is given in black, blue and yellow show the Trials during wet and dry conditions, and ns. Significance levels are indicated by *** for $p < 0.001$, ** for 0.001-0.01, * for 0.01-0.05, (*) for 0.05-0.10, and 'ns' for $p > 0.10$. The model based on IMT data (B) was used to calculate prediction rasters for the days of the field trials (B1, B2).

327

Since the final model trained on IMT data performed slightly better in Trial1 compared to the model trained on SSN data (Figure 7), we chose the IMT model. Using this final random forest model, we generated prediction maps for the days when field trials took place. displays these rasters and reveals significant differences in SWC_{PRED} between Trial1 conducted on March, 2021 and Trial2 conducted on October, 2022.

331

Figure 8: A random forest model was trained to predict soil water content based on spatial and temporal predictor variables. This model was then utilized to make raster predictions for the days when forwarder trials were conducted. The resulting rut depth after four passes is represented by coloured points, while the values of the rasters are displayed using a green to red gradient. Discuss small spatial variability and large temporal variability.

332

4 Discussion

333

3

334

3-14.1 Importance of predictive systems

335

Wet soils are prone to soil disturbances like the formation of deep ruts (McNabb et al., 2001; Poltorak et al., 2018), since water implies a reduction of particle-to-particle bondings within the soil (Hillel, 1998), decreasing the resistance to external

336

337 ~~forces. Consequently, A accurately predicting accurate predictions of~~ soil water content (SWC) and soil trafficability is essential
338 for sustainable forest management and cost-effective, environmentally friendly harvesting operations (Murphy et al., 2007;
339 Vega-Nieva et al., 2009; White et al., 2012; Mohtashami et al., 2017; Mattila and Tokola, 2019; Picchio et al., 2020; Uusitalo
340 et al., 2020). Topographic modelling requires minimal input and the temporal variables used in the final model presented here,
341 are freely available (Copernicus Climate Change Service, 2019). A spatiotemporal model predicting SWC could improve the
342 guidance of machine operators in forest sites during harvesting operations, for example by the effective positioning of brush
343 mats (Labelle and Jaeger, 2018; Labelle et al., 2019). Practical use of static, topographic maps has already been observed in
344 Canada and Scandinavian countries (Ring et al., 2022). By incorporating a temporal aspect, the accuracy of these tools could
345 be further improved. This has the potential to enhance sustainable forest management by protecting soil and mitigating
346 harmful sediment transport (White et al., 2012; Ågren et al., 2015; Kuglerová et al., 2017; Lidberg et al., 2020).

347 3.24.2 Comparison to previous work on predictions of SWC

348 Since soil moisture predictions are crucial for a variety of forestry aspects, several publications have focused on this topic
349 before. ~~In a Swedish case study~~For example, Lidberg et al. (2020) predicted soil moisture classes using spatial models built
350 on topographic indices, correctly classifying 73% of wet areas ~~in a Swedish case study~~. Ågren et al. (2014) reported accurate
351 predictions for 87-92% of observations by comparing soil moisture classes to DTW maps. Larson et al. (2022) used data from
352 the Krycklan catchment and found an accuracy of 84% when comparing moisture classes to the recently developed 'SLU soil
353 moisture map' (Ågren et al., 2021). However, these validations were based on static topographic maps. One attempt to make
354 such static maps dynamic was realized within the DTW concept, which can be customized to calculate various scenarios to
355 adjust to general moisture conditions (e.g., flow initiation areas of 0.25, 1, and 4 ha for wet, moist, and dry conditions,
356 respectively), but selecting the most appropriate scenario during practical use can be a challenging task that requires
357 significant expertise (White et al., 2012; Leach et al., 2017; Lidberg et al., 2020). To overcome this challenge, we aimed for
358 improvement of soil moisture prediction and refined the spatiotemporal approach conceived by Schönauer et al. (2022).
359 During cross-validation of IMT data from sites in Finland, Poland, and parts of the data used in this work, they reported an
360 R^2 of 0.80. The models for the present study showed an R^2 of ~~0.786759±0.13694~~ (SSN) or ~~0.63640±0.0405~~ (IMT),
361 corresponding to Kendall's τ of ~~0.732710±0.095428~~ or ~~0.6202±0.0168~~, respectively. Although this may not seem like an
362 improvement, it should be noted that the data from German sites had less explanatory power of topography for predicting
363 SWC. For example, DTW4 alone explained SWC to a very limited extent ($R^2 = 0.037^{***}$).

364 3.34.3 ~~Comparison to previous work on predicting~~Prediction of rutting

365 Besides the comparisons of SWC with DTW maps, various studies have also investigated the capability of topographic indices
366 in predicting rutting – with conflicting outcomes. For example, Vega-Nieva et al. (2009) found that 65% of ruts deeper than
367 25 cm were located in areas with ~~a vertical proximity to ground water~~a DTW value of less than 1 m, ~~while and~~ 93% of these
368 ~~ruts~~ occurred in areas with DTW values less than 10 m. Similarly, Heppelmann et al. (2022) observed a high frequency of
369 severe rut depth in areas with DTW values less than 1 m in Norway. However, Mohtashami et al. (2017) did not find evidence
370 of such patterns in a field trial where the inclusion of DTW values did not improve the accuracy of a linear model to describe
371 the extents and degrees of rut depth on machine operating trails. In agreement, Schönauer et al. (2021a) found no evidence
372 that DTW or TWI could predict rut depth in a field trial conducted in a temperate broadleaved stand. In this study, ~~we found~~

373 a significant correlation between RD and DTW025 with a Kendall's correlation coefficient (τ) of -0.52***. Yet, this
374 correlation has to be seen with caution: It is mainly driven by differing ranges of RD between the two Trials, as can be seen
375 in Figure 6Figure 6A. We observed that the temporal adjustments of the model based on current moisture conditions could
376 improved predictions of rutting by up-to-date SWC predictions, leading to a τ of 0.61*** (Figure 7B,C). We observed a strong
377 association between rut depth (RD) and predicted values of SWC, with an overall Kendall's correlation coefficient (τ) at 0.63
378 (Figure 7). While no correlation was found between RD and SWC_{PRED} in Trial2, conducted during relatively dry conditions
379 (Figure 3, Figure 7A), a significant correlation was observed during Trial1, on relatively wet conditions. Moreover, the ranges
380 of RD for each trial were consistent with the SWC predictions (), leading to an overall improvement in the goodness-of-fit.
381 While a strong association between RD and predicted values of SWC was observed, the influence of differences between the
382 trials is evident. However, the ranges of RD for each trial were consistent with the SWC predictions. In Trial_{WET}, a significant
383 correlation between RD and SWC_{PRED} was observed (Figure 7B). We hypothesize that the wetter conditions during this trial,
384 which lead to soil destabilization (Hillel, 1998; McNabb et al., 2001), enhanced the predictive power of topographic indices
385 representing soil water distributions. For instance, DTW025 overlapped with surface water in depressions, as observed in the
386 field campaigns for Trial_{WET}.
387 In contrast, during Trial_{DRY}, no correlation was found between RD and SWC_{PRED}. SWC along the measuring sections was
388 likely below the threshold for soils to become susceptible to deformation. For example, Poltorak et al. (2018) stated that ruts
389 only occurred on soils with an SWC above 50%, whereas SWC_{CORE} at Trial_{DRY} was below 30% (Figure 5).

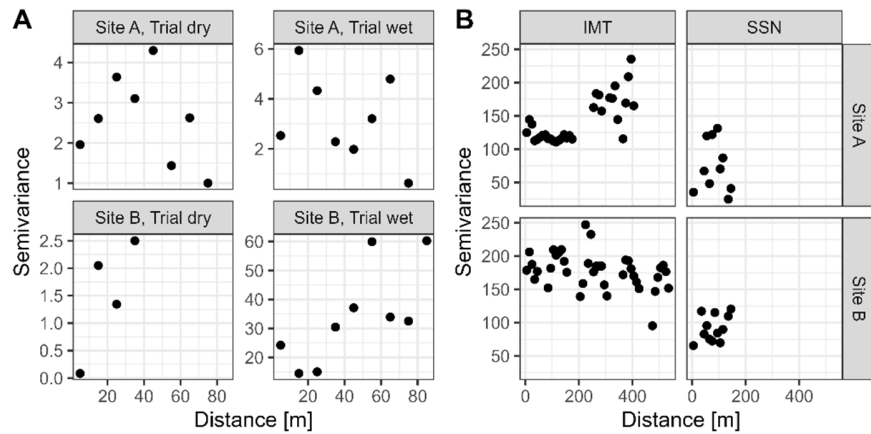
391 **3.4.4.4 Description of the model**

392 The best-performing model in predicting RD incorporated temporal information from SWC_{FRA}L2, Month and Season, as well
393 as -spatial information from DTW025, TWI, SPI and DTW4DTW025, Slope, SPI, TWI and DTW4, as well as temporal
394 information from SWC_{FRA}L2, Month, Season, and was based on data from the manual measurements (IMT). The IMT data
395 was collected in close proximity to the rut depth measurements at Site A (Figure 2), or with a distance of up to 1.3 km at Site
396 B. However, the spatial distance between the IMT training data and the rut depth data did not seem to be crucial for the
397 accuracy of predicting rut depth (Appendix B), since Kendall's τ between RD and SWC_{PRED} was similar for both sites.
398 Soil information was excluded in the initial stages of feature reduction, likely due to the relatively homogenous soil properties
399 on the relatively small study sites. Surprisingly, the correlation between in-situ SWC_{CORE}, sampled directly at the machine
400 operating trails, showed a lower explanatory power in predicting RD than SWC_{PRED}. Although an overall association between
401 RD and SWC_{CORE} was confirmed, no correlation could be found when trials were analysed individually.

402 **4.4.1 Temporal variaton was higher than spatial variation**

403 This indicates that the temporal variability in soil moisture between the trials was more important in this study than the spatial
404 variability within the relatively small areas where each trial was conducted. The spatial distrubition of the rut depth
405 measurements might have been limiting in the present work. The semivariogram indicates the spatial covariation of rut depth
406 and SWC (Figure 88). While the covariation of RD in Sita A is indicated to be high within a range of 10 m (RD-transects
407 were at this distance), on Site B during wet conditions, the sill of the semivariogram reaches almost 40 m, which covered a
408 high number of transects. Similarly, excluding soil information in the initial stages of feature reduction suggests homogeneous

409 soil properties on the relatively small study area.
410 Therefore, we have to admit, that the study design was not ideal for assessing the ability to predict rutting with a spatiotemporal
411 model of SWC, and the results have to be considered with caution.



412 Figure 8. Semivariogram illustrating spatial autocorrelation of (A) rut depth (cm) and (B) soil water content (SWC) across the study
area. Rut depth was measured during two moisture conditions, at four machine operating trail sections, allocated on two sites. The
measuring transects had a spacing of 10 m. SWC was measured with handheld measuring techniques (IMT), or a soil sensor network
(SSN) (Figure 2).

413 The spatiotemporal model (IMT), also supports theis conclusion that spatial variations were wether underrepresented by the
414 study design (or very low compared to temporal variation by nature)-as the temporal feature $SWC_{ERA}L2$ was selected as most
415 important variable and the difference between the model with one predictor variable vs. the final model was small (Figure 4).
416 Still, this slight increase in the models' quality allowed for the integration of spatial patterns and resulted in the significant
417 but vague prediction of RD in Trial_{WET+} ($\tau = 0.3445^*$, Figure 7). Another indication of the integration of spatial patterns can
418 be interpreted by the segregation of the temporal range of the IMT data (2019-2020) and the actual Trials (March 2021 and
419 October 2022, Figure 3), indicating a generalization of spatial and temporal patterns.

420 4.4.2 Most important variables

421 In the final model (IMT), $SWC_{ERA}L2$ has been identified as the most important variable, followed by Month and Season. It is
422 noteworthy that in the data with broader spatial coverage (i.e. IMT), in contrast to the SSN data, dynamic variables took
423 precedence over predictor variables. Surprisingly, when modelling SSN data, characterized by high temporal resolution and
424 low spatial resolution, DTW025 remained the most influential variable. One might have anticipated the opposite, expecting a
425 topographic index to play a central role in modelling IMT data, and dynamic SWC_{ERA} variables dominating the modelling of
426 SSN data.

427 We presume that the low spatial variations of SWC in comparison to temporal variations, inadequately represented by the
428 provided topographic information, may have contributed to this unexpected outcome. Furthermore, the wider spatial coverage
429 in the IMT data likely resulted in more robust averages of SWC, leading to a stronger correlation with the coarse spatial data
430 of ERA5-Land (9x9 km). On the contrary, the SSN data, originating from areas with a size of 100x100 m and known for their
431 temporal wetness, could explain the heightened importance of DTW025. Some sensors might have measured constant water
432 saturation, thereby inflating the explanatory power of topographic information. These assumptions are speculative, and further
433 research in this direction is warranted.

434 In the feature reductions of IMT and SSN data (Figure 4), SWC_{ERA}L2 (7-28 cm soil depth) dominated over SWC_{ERA}L1 (0-7
435 cm). This aligns with in-situ measurements of SWC by the SSN, conducted at a soil depth of approximately 10 cm (Figure
436 3A). Even for the IMT data, where SWC was measured in the top 6 cm of soil, SWC_{ERA}L2 yielded a better goodness-of-fit
437 compared to SWC_{ERA}L1 (Figure 3B). We hypothesize that the prevalence of open lands as the dominant land cover form in
438 the ERA5-Land raster cell (section 2.2.4) contributed to the superior fit of SWC_{ERA}L2. Grasslands typically exhibit higher
439 temporal heterogeneity of soil moisture compared to forests (James et al., 2003). This temporal heterogeneity tends to decrease
440 with deeper soil layers (Tromp-van Meerveld and McDonnell, 2006). Therefore, the stronger correlation between SWC_{ERA}L2
441 and SWC, as well as its higher importance within the random forests, seems reasonable. The disparity between SWC_{ERA} and
442 in-situ SWC can be attributed to the high transpiration rates in forests, as opposed to grass (Kelliher et al., 1993).

443 ~~(James et al., 2003)(Jackson et al., 1997)~~

444 ~~In this study there were negligible differences in performance between the models trained on the IMT dataset and those trained~~
445 ~~on the SSN dataset, with Kendall's τ of 0.63 or 0.64, respectively. However, during Trial1, when the conditions were wetter,~~
446 ~~the correlation between predicted SWC values using the IMT model and RD was slightly stronger. It's worth noting that the~~
447 ~~IMT dataset only required a GPS device and a handheld moisture meter, while the SSN dataset relied on expensive sensor~~
448 ~~networks positioned near the transects where the rutting was observed (Figure 1). Despite this, we argue that manual~~
449 ~~measurements remain an appealing choice for collecting field data and could be facilitated by various forestry stakeholders.~~

450 3.54.5 Further developments

451 The terrain data was derived from a digital elevation model, which is increasingly available for the entire Europe (Hoffmann
452 et al., 2022), while the dynamic variables are based on data and retrievals from ERA5-Land, which are freely available up to
453 ~~three a few~~ days ago. These inputs would allow for automated mapping of current soil water content, which could be made
454 accessible to forestry stakeholders. Recent developments also show a pathway to integrate medium and long range weather
455 forecasts into trafficability predictions, as conceived by the Finnish Meteorological Institute (2023). Both, recent as well as
456 forecasting predictions can lead to, resulting in improved soil protection, higher efficiency of timber harvesting (Suvinen and
457 Saarilahti, 2006), and a new stage of sustainable forest management (Campbell et al., 2013; Jones and Arp, 2019; Uusitalo et
458 al., 2019; D'Acqui et al., 2020). However, it should be noted that the in-situ data of SWC originated from manual
459 measurements, and it was relatively labor-intensive to gather this amount of data. There is potential to reach appropriate
460 accuracy even with a reduced dataset - further investigation would be necessary to determine the essential input data criteria.

461 The alternative to manual measurements is given by sensor networks, which led to comparable results ~~(Figure 7)~~, but such
462 sensor networks are expensive to establish and maintain. Nonetheless, initiatives of installing sensors are emerging and
463 additional manual measurements could be conducted. In the future, forestry stakeholders who require accurate raster
464 predictions could potentially facilitate manual measurements or install sensors ~~(with focus on wet areas)~~ and provide the
465 captured data to scientific organizations, which could deliver spatiotemporal soil moisture predictions in return. The captured
466 data could be made available for creating spatiotemporal models of SWC, allowing for additional training data and daily raster
467 predictions for new areas of interest, with various scientific insights and practical applications.

468
469 ~~In the discussion i think we need to add a section on study design, and that you probably have a lot of spatial covariation in~~
470 ~~your study design, so, you should be careful about overinterpreting any of the "spatial results" as we don't have spatially~~

471 ~~independent samples. I think what you can show is that during dry events you can drive “anywhere”, but during wet conditions~~
472 ~~you get more soil track formation. Figure 2 also suggests that your study sites are near a water divide and dry soils compare~~
473 ~~to the overall wetness of the 9 km square which also includes the valleys. I think that for the aim of the article you limited~~
474 ~~yourself the possibility of detecting any control using the digital terrain indices (eg topography) by the study design (i.e. by~~
475 ~~limiting yourself to a “300 m area”, and relatively flat. Suggest that for future studies this needs to be improved. I think we~~
476 ~~also need to discuss if we should install the 100 new sensor in a better study design for “germany” in our upcoming study?...~~
477 ~~Google semivariogram and , lags and sills. Three rut depth sections are only 100 m long so expect a high autocorrelation.~~

479 **Conclusion**

480 In this study, we developed a spatiotemporal model that used multiple topographic indices, temporal variables, soil moisture
481 retrievals from ERA5-Land, and data from manual measurements to predict soil water content (SWC). Predicted values of
482 SWC were compared to rut depth data collected during four forwarder trials. Overall, the model performed well in predicting
483 rut depth, with a Kendall's τ of 0.613 for all trials. ~~Yet, this result has to be considered with caution, since spatial covariation~~
484 ~~was detected in parts. We hope, that this experience helps for future research, in which more attention to spatial covariation~~
485 ~~on soils should be paid. Still, we believe that a dynamic prediction of SWC will~~~~This predictive capability could~~ help forest
486 managers and machine operators avoid wet areas, leading to more sustainable forest operations. Using freely available
487 temporal information is a significant improvement, as it enables more accurate and up-to-date predictions, which allow to
488 make more informed decisions and avoid potential hazards. Future work should focus ~~on developing automated pathways~~
489 ~~for generating daily raster predictions of SWC, and on generating reliable and comprehensive in-situ data, enabling day-to-~~
490 ~~day prediction rasters to be supplied and used. However, it should be noted that the models used are always limited by the~~
491 ~~available data to be trained on. Therefore, t.~~ There is a need for more data ~~on rutting and SWC, measured with a sufficient~~
492 ~~spatial coverage, whether~~ by manual measurements, ~~or~~ the establishment of additional sensor networks, ~~or by automatic~~
493 ~~ways of capturing rut depth data through machines driving off-road,~~ to cover more areas and different sites and regions.
494 ~~Additionally, the model's predictive accuracy could be improved by obtaining more data on rut depth, which could be captured~~
495 ~~automatically by machines driving off road.~~

496 **Data availability**

497 The data used in this work will be made accessible via Zenodo

498 **Author contribution**

499 MS and DJ designed the experiments and MS and FH carried them out. MS developed the model code and performed the
500 simulations. MS prepared the manuscript with contributions from all co-authors.

501 **Competing interests**

502 The authors declare that they have no conflict of interest.

503 **Acknowledgements**

504 We acknowledge the financial support from the Eva Mayr-Stihl Stiftung for this work. We extend our gratitude to the
505 Geological Survey of Northrhine-Westphalia (Landesbetrieb NRW) for conducting the soil mapping on the experimental sites
506 and for their contributions to the field trials analysis. In particular, we would like to thank Dr. Heinz Peter Schrey, Dirk Elhaus,

507 Thilo Simon, and Rainer Janssen. Our appreciation also goes to the Forest Education Centre, Forstliches Bildungszentrum,
508 Zentrum für Wald und Holzwirtschaft, Landesbetrieb Wald und Holz NRW, Arnsberg, Germany, for their valuable support
509 during the fieldwork. Special thanks to Thilo Wagner and Thomas Späthe for their efforts in organizing the field trials, and to
510 Michael Schulte for operating the forwarder. ChatGPT (OpenAI, San Francisco, CA, USA) provided assistance in sentence
511 editing – all content was generated solely by the authors.

512 **Funding**

513 This work was supported by the cooperation project “BefahrGut” funded by the State of North Rhine-Westphalia, Germany,
514 through its Forest Education Centre, Forstliches Bildungszentrum, Zentrum für Wald und Holzwirtschaft, Landesbetrieb Wald
515 und Holz NRW, Arnsberg, Germany; by the Bio Based Industries Joint Undertaking under the European Union’s Horizon
516 2020 research and innovation program, TECH4EFFECT Knowledge and Technologies for Effective Wood Procurement—
517 project, [grant number 720757].

518

519

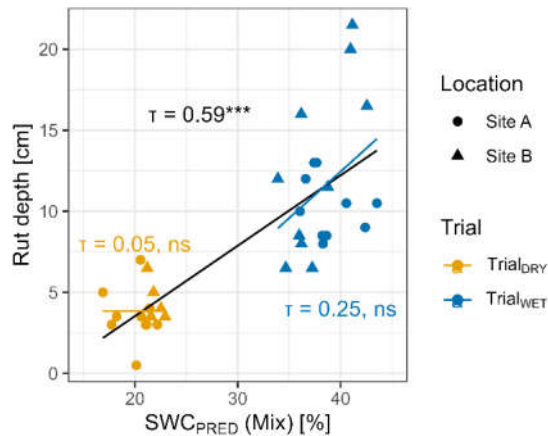
520 **45 Appendix**

521 **Appendix A**

522 To model the dataset consisting of both IMT and SSN data, the procedure described in section 2 was followed. The IMT
523 dataset was merged with a subsample of the SSN dataset, where the sample size of the SSN part was twice that of the IMT
524 dataset. This was done to prevent over-weighting of the SSN dataset. The resulting combination of IMT and SSN data was
525 called the "Mix" dataset.

526 The final model using the Mix dataset included the input variables SWC_{ERA}L2, Month, TWI, SWC_{ERA}L1, DTW025, Season,
527 DTW1 and DTW4~~SWC_{ERA}L2, Month, TWI, Year, SWC_{ERA}L1, Season, DTW025, DTW2, Slope, SPI, and Accumulation,~~
528 and achieved a τ of 0.6559 ± 0.0814 (which corresponded to R^2 values of 0.6395 ± 0.10817). Appendix A Supplementary Figure
529 1 shows that the correlation between the model outputs (SWC_{PRED}) and rut depth (RD) was significant.

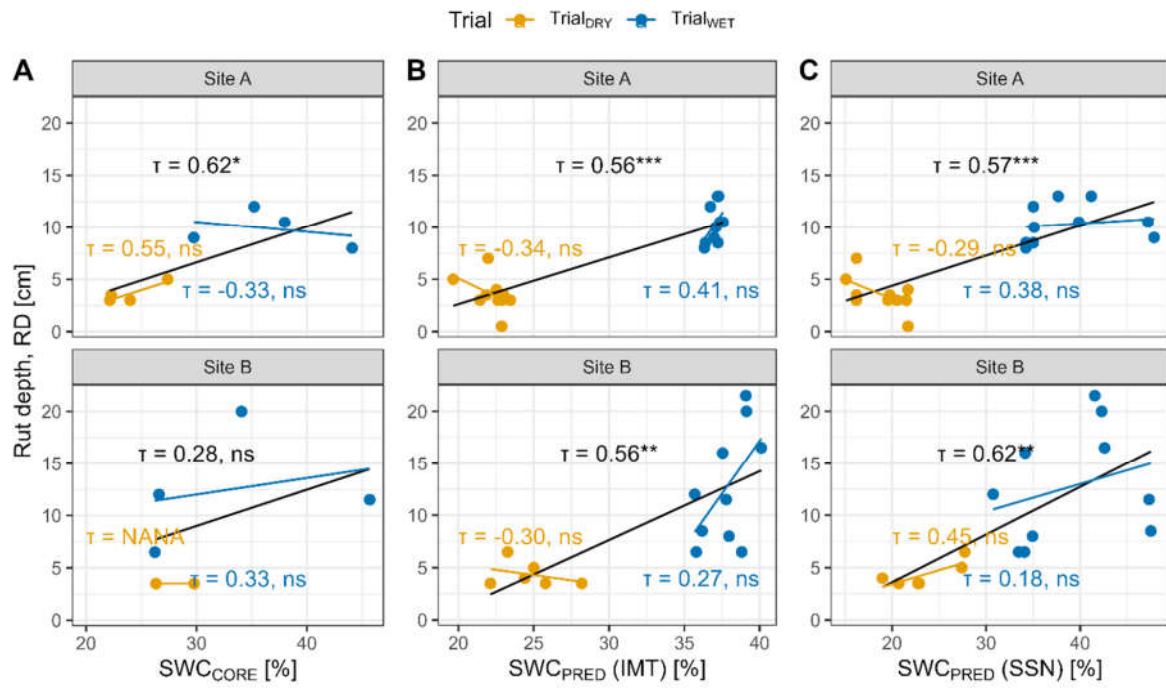
530 Since the models trained on the Mix dataset did not perform better than those trained on the IMT or SSN datasets, we did not
531 investigate the fused data partition any further, as one research question addressed the use of different data origins. For future
532 work, however, the fused data would provide additional information, as compared to the individual datasets.



533

Supplementary Figure 1: Rut depth (RD) was determined after four passes of a forwarder, driving on two Sites (1A and 2B), during two seasons (Trial_{WET}1 and Trial_{DRY}2). RD was compared to SWC values predicted by a random forest model trained on data from manual measurements or captured through a continuously measuring soil sensor network ('Mix'). Correlations were evaluated using Kendall's τ and significance levels are indicated by *** for $p < 0.001$, ** for 0.001-0.01, * for 0.01-0.05, (*) for 0.05-0.10, and 'ns' for $p > 0.10$.

534



Supplementary Figure 2. Rut depth (RD) was determined after four passes of a forwarder, driving on two Sites (A and B, Figure 2), during two seasons (Trial_{WET} and Trial_{DRY}, conducted under different moisture conditions). RD was compared to SWC values, determined for undisturbed soil cores (A) and SWC values predicted by a random forest model trained on manually obtained IMT measurements (B, see Figure 1) and predicted by a model trained data from a continuously measuring soil sensor network (SSN, C). Correlations were evaluated using Kendall's τ . The correlation of all values is given in black, blue and yellow show the Trials during wet and dry conditions. Significance levels are indicated by *** for $p < 0.001$, ** for 0.001-0.01, * for 0.01-0.05, (*) for 0.05-0.10, and 'ns' for $p > 0.10$.

537 **56** REFERENCES

- 538 Ågren, A., Larson, J., Paul, S. S., Laudon, H., and Lidberg, W. (2021). Use of multiple LIDAR-derived digital terrain indices
539 and machine learning for high-resolution national-scale soil moisture mapping of the Swedish forest landscape. *Geoderma*
540 404, 115280. doi: 10.1016/j.geoderma.2021.115280
- 541 Ågren, A., Lidberg, W., and Ring, E. (2015). Mapping Temporal Dynamics in a Forest Stream Network—Implications for
542 Riparian Forest Management. *Forests* 6, 2982–3001. doi: 10.3390/f6092982
- 543 Ågren, A., Lidberg, W., Strömberg, M., Ogilvie, J., and Arp, P. (2014). Evaluating digital terrain indices for soil wetness
544 mapping – a Swedish case study. *Hydrology and Earth System Sciences* 18, 3623–3634. doi: 10.5194/hess-18-3623-2014
- 545 Ala-Ilomäki, J., Lindeman, H., Mola-Yudego, B., Prinz, R., Väättäinen, K., Talbot, B., et al. (2021). The effect of bogie track
546 and forwarder design on rut formation in a peatland. *International Journal of Forest Engineering* 45, 1–8. doi:
547 10.1080/14942119.2021.1935167
- 548 Allman, M., Jankovský, M., Messingerová, V., and Allmanová, Z. (2017). Soil moisture content as a predictor of soil
549 disturbance caused by wheeled forest harvesting machines on soils of the Western Carpathians. *Journal of Forestry*
550 *Research* 28, 283–289. doi: 10.1007/s11676-016-0326-y
- 551 Ampoorter, E., van Nevel, L., Vos, B. de, Hermy, M., and Verheyen, K. (2010). Assessing the effects of initial soil
552 characteristics, machine mass and traffic intensity on forest soil compaction. *Forest Ecology and Management* 260, 1664–
553 1676. doi: 10.1016/j.foreco.2010.08.002
- 554 Awaida, A., and Westervelt, J. (2020). Geographic Resources Analysis Support System (GRASS GIS). USA: Geographic
555 Resources Analysis Support System (GRASS GIS) Software, <https://grass.osgeo.org>
- 556 Beylich, A., Oberholzer, H.-R., Schrader, S., Höper, H., and Wilke, B.-M. (2010). Evaluation of soil compaction effects on
557 soil biota and soil biological processes in soils. *Soil and Tillage Research* 109, 133–143. doi: 10.1016/j.still.2010.05.010
- 558 Bezirksregierung Köln (2020). *Digitales Geländemodell DGMI [Digital elevation model]*. Accessed November 08, 2021,
559 [https://www.bezreg-koeln.nrw.de/brk_internet/
560 geobasis/hoehenmodelle/digitale_gelaendemodelle/gelaendemodell/index.html](https://www.bezreg-koeln.nrw.de/brk_internet/geobasis/hoehenmodelle/digitale_gelaendemodelle/gelaendemodell/index.html)
- 561 Bezirksregierung Köln (2023). *Landbedeckung NRW*. Accessed November 16, 2023, [https://www.bezreg-
562 koeln.nrw.de/geobasis-nrw/produkte-und-dienste/luftbild-und-satellitenbildinformationen/aktuelle-luftbild-und-3](https://www.bezreg-koeln.nrw.de/geobasis-nrw/produkte-und-dienste/luftbild-und-satellitenbildinformationen/aktuelle-luftbild-und-3)
- 563 Bivand, R. S. (2021). rgrass7: Interface Between GRASS 7 Geographical Information System and R, [https://CRAN.R-
564 project.org/package=rgrass7](https://CRAN.R-project.org/package=rgrass7)
- 565 Breiman, L. (2001). Random forests. *Machine Learning* 45, 5–32. doi: 10.1023/A:1010933404324
- 566 Cambi, M., Certini, G., Neri, F., and Marchi, E. (2015). The impact of heavy traffic on forest soils: A review. *Forest Ecology*
567 *and Management* 338, 124–138. doi: 10.1016/j.foreco.2014.11.022
- 568 Campbell, D. M.H., White, B., and Arp, P. (2013). Modeling and mapping soil resistance to penetration and rutting using
569 LiDAR-derived digital elevation data. *Journal of Soil and Water Conservation* 68, 460–473. doi: 10.2489/jswc.68.6.460
- 570 Carranza, C., Nolet, C., Pezij, M., and van der Ploeg, M. (2021). Root zone soil moisture estimation with Random Forest.
571 *Journal of Hydrology* 593, 125840. doi: 10.1016/j.jhydrol.2020.125840
- 572 Cavalli, A., Francini, S., McRoberts, R. E., Falanga, V., Congedo, L., Fioravante, P. de, et al. (2023). Estimating Afforestation
573 Area Using Landsat Time Series and Photointerpreted Datasets. *Remote Sensing* 15, 923. doi: 10.3390/rs15040923
- 574 Chen, T., He, T., Benesty, M., Khotilovich, V., Tang, Y., Cho, H., et al. (2021). *xgboost: Extreme Gradient Boosting*.

575 Accessed November 09, 2021, <https://CRAN.R-project.org/package=xgboost>

576 Copernicus Climate Change Service (2019). *ERA5-Land hourly data from 2001 to present*. ECMWF.

577 Crawford, L. J., Heinse, R., Kimsey, M. J., and Page-Dumroese, D. S. (2021). Soil Sustainability and Harvest Operations.
578 *General Technical Report RMRS*. doi: 10.2737/RMRS-GTR-421

579 Curzon, M. T., Slesak, R. A., Palik, B. J., and Schwager, J. K. (2022). Harvest impacts to stand development and soil properties
580 across soil textures: 25-year response of the aspen Lake States LTSP installations. *Forest Ecology and Management* 504,
581 119809. doi: 10.1016/j.foreco.2021.119809

582 D'Acqui, L. P., Certini, G., Cambi, M., and Marchi, E. (2020). Machinery's impact on forest soil porosity. *Journal of*
583 *Terramechanics* 91, 65–71. doi: 10.1016/j.jterra.2020.05.002

584 DeArmond, D., Ferraz, J., and Higuchi, N. (2021). Natural Recovery of Skid Trails. A Review. *Canadian Journal of Forest*
585 *Research*. doi: 10.1139/cjfr-2020-0419

586 Eijkelkamp Agrisearch Equipment (2013). *User Manual for the Moisture Meter type HH2*. Accessed August 07, 2020,
587 https://www.eijkelkamp.com/download.php?file=M1142602e_Soil_moisture_meter_flab.pdf

588 Eliasson, L. (2005). Effects of forwarder tyre pressure on rut formation and soil compaction. *Silva Fennica* 39, 549–557. doi:
589 10.14214/sf.366

590 Finnish Meteorological Institute (2023). *Harvester Seasons*. Accessed November 08, 2023,
591 https://harvesterseasons.com/HarvesterSeasons_Description2pager_v2.pdf

592 Francesca, V., Osvaldo, F., Stefano, P., and Paola, R. P. (2010). Soil Moisture Measurements: Comparison of Instrumentation
593 Performances. *J. Irrig. Drain Eng.* 136, 81–89. doi: 10.1061/(ASCE)0733-9437(2010)136:2(81)

594 Gröll, M. (2011). Den Waldboden schonen–Vorsorgender Bodenschutz beim Einsatz von Holzerntetechnik [Soil protection
595 in forest operations]. *Eberswalder Forstliche Schriftenreihe* 47, 37–44.

596 Guo, M., Li, J., Sheng, C., Xu, J., and Wu, L. (2017). A Review of Wetland Remote Sensing. *Sensors (Basel)* 17. doi:
597 10.3390/s17040777

598 Hansson, L., Šimůnek, J., Ring, E., Bishop, K., and Gärdenäs, A. I. (2019). Soil Compaction Effects on Root-Zone Hydrology
599 and Vegetation in Boreal Forest Clearcuts. *Soil Sci. Soc. Am. j.* 83, 239. doi: 10.2136/sssaj2018.08.0302

600 Hauglin, M., Rahlf, J., Schumacher, J., Astrup, R., and Breidenbach, J. (2021). Large scale mapping of forest attributes using
601 heterogeneous sets of airborne laser scanning and National Forest Inventory data. *Forest Ecosystems* 8, 65. doi:
602 10.1186/s40663-021-00338-4

603 Heppelmann, J. B., Talbot, B., Antón Fernández, C., and Astrup, R. (2022). Depth-to-water maps as predictors of rut severity
604 in fully mechanized harvesting operations. *International Journal of Forest Engineering* 33, 108–118. doi:
605 10.1080/14942119.2022.2044724

606 Heubaum, F. (2015). *Bodenschutz im Staatsbetrieb Sachsenforst [Soil protection]: Projekte zur Technologieerprobung*.
607 Accessed November 05, 2021, https://www.sbs.sachsen.de/download/Bodenschutz_Projekte_2015_09_30.pdf

608 Hijmans, R. J. (2020). raster: Geographic Data Analysis and Modeling, <https://CRAN.R-project.org/package=raster>

609 Hillel, D. (1998). *Environmental soil physics: Fundamentals, applications, and environmental considerations*. San Diego,
610 California: Elsevier.

611 Hoffmann, S., Schönauer, M., Heppelmann, J., Asikainen, A., Cacot, E., Eberhard, B., et al. (2022). Trafficability Prediction
612 Using Depth-to-Water Maps: the Status of Application in Northern and Central European Forestry. *Curr Forestry Rep* 338,

613 124. doi: 10.1007/s40725-021-00153-8

614 Horn, R., Vossbrink, J., Peth, S., and Becker, S. (2007). Impact of modern forest vehicles on soil physical properties. *Forest*
615 *Ecology and Management* 248, 56–63. doi: 10.1016/j.foreco.2007.02.037

616 James, S. E., Pärtel, M., Wilson, S. D., and Peltzer, D. A. (2003). Temporal heterogeneity of soil moisture in grassland and
617 forest. *Journal of Ecology*, 234–239.

618 Jones, M.-F., and Arp, P. (2017). Relating Cone Penetration and Rutting Resistance to Variations in Forest Soil Properties
619 and Daily Moisture Fluctuations. *Open Journal of Soil Science* 07, 149–171. doi: 10.4236/ojss.2017.77012

620 Jones, M.-F., and Arp, P. (2019). Soil Trafficability Forecasting. *Open Journal of Forestry* 9, 296–322. doi:
621 10.4236/ojf.2019.94017

622 Kelliher, F. M., Leuning, R., and Schulze, E. D. (1993). Evaporation and canopy characteristics of coniferous forests and
623 grasslands. *Oecologia* 95, 153–163. doi: 10.1007/BF00323485

624 Kempainen, J., Niittynen, P., Riihimäki, H., and Luoto, M. (2018). Modelling soil moisture in a high-latitude landscape using
625 LiDAR and soil data. *Earth Surf. Process. Landforms* 43, 1019–1031. doi: 10.1002/esp.4301

626 Koen Hufkens, Reto Stauffer, and Elio Campitelli (2019). *khufkens/ecmwfr: ecmwfr*. Zenodo.

627 Kristensen, J. A., Balstrøm, T., Jones, R. J. A., Jones, A., Montanarella, L., Panagos, P., et al. (2019). Development of a
628 harmonised soil profile analytical database for Europe: a resource for supporting regional soil management. *SOIL* 5, 289–
629 301. doi: 10.5194/soil-5-289-2019

630 Kuglerová, L., Hasselquist, E. M., Richardson, J. S., Sponseller, R. A., Kreuzweiser, D. P., and Laudon, H. (2017).
631 Management perspectives on *Aqua incognita* : Connectivity and cumulative effects of small natural and artificial streams
632 in boreal forests. *Hydrological Processes* 31, 4238–4244. doi: 10.1002/hyp.11281

633 Kuhn, M. (2020). *caret: Classification and Regression Training*. Accessed November 09, 2021, [https://CRAN.R-](https://CRAN.R-project.org/package=caret)
634 [project.org/package=caret](https://CRAN.R-project.org/package=caret)

635 Kursa, M. B., and Rudnicki, W. R. (2010). Feature Selection with the Boruta Package. *J. Stat. Soft.* 36. doi:
636 10.18637/jss.v036.i11

637 Labelle, E. R., and Jaeger, D. (2018). Management Implications of Using Brush Mats for Soil Protection on Machine
638 Operating Trails during Mechanized Cut-to-Length Forest Operations. *Forests* 10, 19. doi: 10.3390/f10010019

639 Labelle, E. R., Poltorak, B. J., and Jaeger, D. (2019). The role of brush mats in mitigating machine-induced soil disturbances:
640 An assessment using absolute and relative soil bulk density and penetration resistance. *Canadian Journal of Forest*
641 *Research* 49, 164–178. doi: 10.1139/cjfr-2018-0324

642 Lal, P., Singh, G., Das, N. N., Colliander, A., and Entekhabi, D. (2022). Assessment of ERA5-Land Volumetric Soil Water
643 Layer Product Using In Situ and SMAP Soil Moisture Observations. *IEEE Geosci. Remote Sensing Lett.* 19, 1–5. doi:
644 10.1109/LGRS.2022.3223985

645 Larson, J., Lidberg, W., Ågren, A. M., and Laudon, H. (2022). *Predicting soil moisture conditions across a heterogeneous*
646 *boreal catchment using terrain indices*.

647 Leach, J. A., Lidberg, W., Kuglerová, L., Peralta-Tapia, A., Ågren, A., and Laudon, H. (2017). Evaluating topography-based
648 predictions of shallow lateral groundwater discharge zones for a boreal lake-stream system. *Water Resources Research* 53,
649 5420–5437. doi: 10.1002/2016WR019804

650 Lidberg, W., Nilsson, M., and Ågren, A. (2020). Using machine learning to generate high-resolution wet area maps for

651 planning forest management: A study in a boreal forest landscape. *Ambio* 49, 475–486. doi: 10.1007/s13280-019-01196-9

652 Mattila, U., and Tokola, T. (2019). Terrain mobility estimation using TWI and airborne gamma-ray data. *Journal of*

653 *environmental management* 232, 531–536. doi: 10.1016/j.jenvman.2018.11.081

654 McNabb, D. H., Startsev, A. D., and Nguyen, H. (2001). Soil Wetness and Traffic Level Effects on Bulk Density and Air-

655 Filled Porosity of Compacted Boreal Forest Soils. *Soil Science Society of America Journal* 65, 1238–1247. doi:

656 10.2136/sssaj2001.6541238x

657 Mohtashami, S., Eliasson, L., Jansson, G., and Sonesson, J. (2017). Influence of soil type, cartographic depth-to-water, road

658 reinforcement and traffic intensity on rut formation in logging operations: a survey study in Sweden. *Silva Fennica* 51. doi:

659 10.14214/sf.2018

660 Moore, I. D., Grayson, R. B., and Ladson, A. R. (1991). Digital terrain modelling: A review of hydrological,

661 geomorphological, and biological applications. *Hydrol. Process.* 5, 3–30. doi: 10.1002/hyp.3360050103

662 Muñoz-Sabater, J., Dutra, E., Agustí-Panareda, A., Albergel, C., Arduini, G., Balsamo, G., et al. (2021). ERA5-Land: a state-

663 of-the-art global reanalysis dataset for land applications. *Earth Syst. Sci. Data* 13, 4349–4383. doi: 10.5194/essd-13-4349-

664 2021

665 Murphy, P. N. C., Ogilvie, J., and Arp, P. (2009). Topographic modelling of soil moisture conditions: A comparison and

666 verification of two models. *European Journal of Soil Science* 60, 94–109. doi: 10.1111/j.1365-2389.2008.01094.x

667 Murphy, P. N. C., Ogilvie, J., Connor, K., and Arp, P. (2007). Mapping wetlands: A comparison of two different approaches

668 for New Brunswick, Canada. *WETLANDS* 27, 846–854. doi: 10.1672/0277-5212(2007)27[846:MWACOT]2.0.CO;2

669 Murphy, P. N. C., Ogilvie, J., Meng, F.-R., White, B., Bhatti, J. S., and Arp, P. (2011). Modelling and mapping topographic

670 variations in forest soils at high resolution: A case study. *Ecological Modelling* 222, 2314–2332. doi:

671 10.1016/j.ecolmodel.2011.01.003

672 Oliveira, V. A., Rodrigues, A. F., Morais, M. A. V., Terra, M. d. C. N. S., Guo, L., and Mello, C. R. (2021). Spatiotemporal

673 modelling of soil moisture in an Atlantic forest through machine learning algorithms. *Eur J Soil Sci* 72, 1969–1987. doi:

674 10.1111/ejss.13123

675 Picchio, R., Latterini, F., Mederski, P. S., Tocci, D., Venanzi, R., Stefanoni, W., et al. (2020). Applications of GIS-Based

676 Software to Improve the Sustainability of a Forwarding Operation in Central Italy. *Sustainability* 12, 5716. doi:

677 10.3390/su12145716

678 Poltorak, B. J., Labelle, E. R., and Jaeger, D. (2018). Soil displacement during ground-based mechanized forest operations

679 using mixed-wood brush mats. *Soil and Tillage Research* 179, 96–104. doi: 10.1016/j.still.2018.02.005

680 Quinn, P., Beven, K., Chevallier, P., and Planchon, O. (1991). The prediction of hillslope flow paths for distributed

681 hydrological modelling using digital terrain models. *Hydrol. Process.* 5, 59–79. doi: 10.1002/hyp.3360050106

682 R Core Team (2023). *R: A Language and Environment for Statistical Computing*. Vienna, Austria: The R Foundation for

683 Statistical Computing.

684 Ring, E., Ågren, A., Bergkvist, I., Finér, L., Johansson, F., and Högbom, L. (2022). *A guide to using wet area maps in forestry:*

685 *En guide för hur man kan använda markfuktighetskartor i skogsbruket*. ARBETSRAPPORT 1051-2020. Uppsala, Sweden.

686 Schönauer, M., Hoffmann, S., Maack, J., Jansen, M., and Jaeger, D. (2021a). Comparison of Selected Terramechanical Test

687 Procedures and Cartographic Indices to Predict Rutting Caused by Machine Traffic during a Cut-to-Length Thinning

688 Operation. *Forests* 12, 113. doi: 10.3390/f12020113

689 Schönauer, M., and Maack, J. (2021). R-code for calculating depth-to-water (DTW) maps using GRASS GIS (Version v1).
690 *Zenodo*. doi: 10.5281/zenodo.5638518

691 Schönauer, M., Prinz, R., Väätäinen, K., Astrup, R., Pszenny, D., Lindeman, H., et al. (2022). Spatio-temporal prediction of
692 soil moisture using soil maps, topographic indices and SMAP retrievals. *International Journal of Applied Earth
693 Observation and Geoinformation* 108, 102730. doi: 10.1016/j.jag.2022.102730

694 Schönauer, M., Väätäinen, K., Prinz, R., Lindeman, H., Pszenny, D., Jansen, M., et al. (2021b). Spatio-temporal prediction
695 of soil moisture and soil strength by depth-to-water maps. *International Journal of Applied Earth Observation and
696 Geoinformation* 105, 102614. doi: 10.1016/j.jag.2021.102614

697 Sirén, M., Salmivaara, A., Ala-Ilomäki, J., Launiainen, S., Lindeman, H., Uusitalo, J., et al. (2019). Predicting forwarder rut
698 formation on fine-grained mineral soils. *Scandinavian Journal of Forest Research* 34, 145–154. doi:
699 10.1080/02827581.2018.1562567

700 Sørensen, R., and Seibert, J. (2007). Effects of DEM resolution on the calculation of topographical indices: TWI and its
701 components. *Journal of Hydrology* 347, 79–89. doi: 10.1016/j.jhydrol.2007.09.001

702 Suvinen, A., and Saarilhti, M. (2006). Measuring the mobility parameters of forwarders using GPS and CAN bus techniques.
703 *Journal of Terramechanics* 43, 237–252. doi: 10.1016/j.jterra.2005.12.005

704 Tromp-van Meerveld, H. J., and McDonnell, J. J. (2006). On the interrelations between topography, soil depth, soil moisture,
705 transpiration rates and species distribution at the hillslope scale. *Advances in Water Resources* 29, 293–310. doi:
706 10.1016/j.advwatres.2005.02.016

707 Uusitalo, J., Ala-Ilomäki, J., Lindeman, H., Toivio, J., and Sirén, M. (2019). Modelling soil moisture – soil strength
708 relationship of fine-grained upland forest soils. *Silva Fennica* 53. doi: 10.14214/sf.10050

709 Uusitalo, J., Ala-Ilomäki, J., Lindeman, H., Toivio, J., and Sirén, M. (2020). Predicting rut depth induced by an 8-wheeled
710 forwarder in fine-grained boreal forest soils. *Annals of forest science* 77. doi: 10.1007/s13595-020-00948-y

711 Vega-Nieva, D. J., Murphy, P. N. C., Castonguay, M., Ogilvie, J., and Arp, P. (2009). A modular terrain model for daily
712 variations in machine-specific forest soil trafficability. *Canadian Journal of Soil Science* 89, 93–109. doi:
713 10.4141/CJSS06033

714 Walker, J. P., Willgoose, G. R., and Kalma, J. D. (2004). In situ measurement of soil moisture: a comparison of techniques.
715 *Journal of Hydrology* 293, 85–99. doi: 10.1016/j.jhydrol.2004.01.008

716 White, B., Ogilvie, J., Campbell, D. M.H., Hiltz, D., Gauthier, B., Chisholm, H. K., et al. (2012). Using the Cartographic
717 Depth-to-Water Index to Locate Small Streams and Associated Wet Areas across Landscapes. *Canadian Water Resources
718 Journal* 37, 333–347. doi: 10.4296/cwrj2011-909

719 Wright, M. N., and Ziegler, A. (2017). ranger: A Fast Implementation of Random Forests for High Dimensional Data in C++
720 and R. *J. Stat. Soft.* 77. doi: 10.18637/jss.v077.i01

721